

# All-optical steering of light via spatial Bloch oscillations in a gas of three-level atoms

Chao Hang<sup>1,2</sup> and V. V. Konotop<sup>1,3</sup>

<sup>1</sup>*Centro de Física Teórica e Computacional, Universidade de Lisboa,  
Complexo Interdisciplinar, Avenida Professor Gama Pinto 2, Lisboa 1649-003, Portugal*

<sup>2</sup>*Department of Physics, East China Normal University, Shanghai 200062, China*

<sup>3</sup>*Departamento de Física, Faculdade de Ciências, Universidade de Lisboa,  
Campo Grande, Edifício C8, Piso 6, Lisboa 1749-016, Portugal*

A standing-wave control field applied to a three-level atomic medium in a planar hollow-core photonic crystal waveguide creates periodic variations of linear and nonlinear refractive indexes of the medium. This property can be used for efficient steering of light. In this work we study, both analytically and numerically, the dynamics of probe optical beams in such structures. By properly designing the spatial dependence of the nonlinearity it is possible to induce long-living Bloch oscillations of spatial gap solitons, thus providing desirable change in direction of the beam propagation without inducing appreciable diffraction. Due to the significant enhancement of the nonlinearity, such self-focusing of the probe beam can be reached at extremely weak light intensities.

PACS numbers: 42.65.Tg, 05.45.Yv, 42.50.Gy

## I. INTRODUCTION

Beam steering is one of the most important technologies in the modern optics due to its numerous applications in such fields as optical imaging, laser machining, and free space communication. Various physical mechanisms have been explored for deflection of beams by inducing refractive index gradient [1]. They include mechanical motion [2], thermal gradient [3], the acousto-optical interaction [4], and the electro-optic effect [5]. Fast beam steering in photonic crystals [6] and phased arrays [7] were also proposed.

The direction of the light propagation can also be changed by another beam of light through interaction with matter. In particular, a medium exhibiting electromagnetically induced transparency (EIT) [8] can provide large probe-beam deflection since the refractive index changes significantly near the transparency center [9]. Among the related studies we mention the refractive index measurements by probe-beam [10], investigation of slow light deflection by magneto-optically controlled atomic media [11], and exploring a scheme of all-optical beam steering [12]. Yet another example is the electromagnetically induced waveguiding which uses the control field as a waveguide to confine the probe field [13].

However, the schemes proposed in the most of the previous studies are restricted to the linear regime. They usually result in a spread of the probe pulse because the refractive index gradient depends on both the probe frequency and the spatial coordinates. Fortunately, such spread can be suppressed by the enhancement of the wave localization through the formation of solitons. Large intrinsic nonlinearity in an EIT-based media allows for existence of probe beam solitons with extremely weak light intensities [14]. More specifically, ultraslow solitons [15], spatial solitons [16], and gap solitons [17] at low light intensity can exist in such kind of media.

In this work, we propose a scheme to achieve efficient all-optical steering of light in a resonant three-level

atomic system under EIT regime. The scheme is based on the phenomenon of nonlinear long-living Bloch oscillations (BOs) of gap solitons, recently reported in Ref. [18]. The system at hand is a gas of  $\Lambda$ -atoms loaded in a planar waveguide created by two photonic crystals. The control field used in the system is a standing-wave laser beam that originates a linear force, as well as *linear* and *nonlinear* optical lattices (OLs) affecting a weak probe beam. OLs in such a system are flexible: their parameters can be adjusted either by changing the geometry and/or intensity of the control field, or by varying one- and/or two-photon detunings.

Briefly, the mechanism of the steering consists of two ingredients: the spatially periodic linear force induces dynamics of the probe beam in the transverse direction, while the combined effect of the lattices controls the direction of the beam propagation introducing desirable and controllable deviations. More specifically, the linear OL provides the band structure necessary for existence of the Bloch states, while the nonlinear lattice is used to control the stability properties of the Bloch states necessary for existence of gap solitons at both edges of each band [18]. Due to the enhancement of the Kerr nonlinearity induced by the EIT mechanism, stable spatial gap solitons, representing the beam channels, can be formed even subject to extremely weak probe light intensity and subsequently strongly deflected without undergoing appreciable deformations and attenuations.

The paper is organized as follows. In the next section, the model is introduced. In Sec. III, the nonlinear equation governing the evolution of the probe field amplitude is derived. We show that stable spatial gap solitons can exist under properly chosen parameters of the control field. We also show how one can implement an efficient all-optical steering of the gap solitons. All results in this work are obtained under a set of experimentally feasible parameters. The outcomes are summarized in the Conclusion.

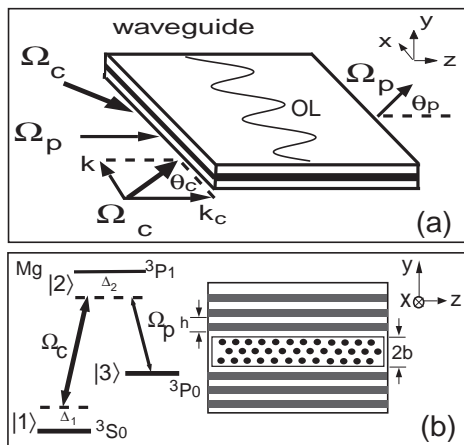


FIG. 1: (a) The geometry considered in the present work: the direction of propagation of the probe beam ( $z$ -direction) is orthogonal to the OL axis ( $x$ -direction).  $\theta_c = \arctan(k/k_c)$  is the half angle between the two input control beams and  $\theta_p$  is the output angle of the probe beam. (b) Left panel:  $\Lambda$ -type atomic system interacting with two laser beams.  $\Omega_p$  and  $\Omega_c$  are respectively the Rabi frequencies of the probe and control fields.  $\Delta_1$  and  $\Delta_2$  are respectively the two-photon and the one-photon detunings. Right panel: The waveguide cross section. The dotted region denotes the core filled with the atomic gas and limited by the Bragg mirrors.  $2b$ ,  $h_a$ , and  $h_b$  are the thicknesses of the core and different materials of the Bragg mirrors, respectively.

## II. THE MODEL

### A. Preliminary arguments

We consider a cold gas of lifetime-broadened  $\Lambda$ -type atoms, loaded into an anti-relaxation-coated planar hollow-core photonic crystal waveguide, schematically shown in Fig. 1. (It is relevant to note that both room-temperature and ultracold atoms have been successfully loaded into hollow-core photonic crystal fibers [19], and have further been used to study EIT [20] and all-optical switching [21]). As in any  $\Lambda$ -system, the atoms can populate three states: the ground state  $|1\rangle$ , the excited state  $|2\rangle$ , and the low-energy state  $|3\rangle$  [see Fig. 1 (b)]. The transitions between the states  $|1\rangle$  and  $|3\rangle$  are forbidden.

For the particular choice of the atomic gas and geometry of the system, we take into account the two facts. First, in order to contribute to the nonlinear polarization the matrix elements of the transition between the lower states and the excited state must be nonzero, and hence the population of the excited state must also be nonzero (see e.g. [17]). Thus, one has to explore a gas with weak atomic losses due to spontaneous emission from the excited state. A particular system having such properties is the laser-cooled alkaline earth metal atoms, such as strontium atoms [22] where the atomic states  $|1\rangle$ ,  $|2\rangle$ , and  $|3\rangle$  can be chosen as  $^1S_0$ , and  $^3P_1$ , and  $^3P_0$ , respectively. One of the advantages of such a system is that

the atoms possess a long life time even in their excited states: the life time of the state  $|2\rangle$  is about  $21.3 \mu\text{s}$  corresponding to the decay rate 47 kHz. Therefore, in what follows we use this system for the sake of the numerical studies (see Figs. 2, 3, and 4).

The second fact to be taken into account is the smallest possible size of the system. Our aim is to execute effective steering of light using OLs. In order to make the periodicity appreciable in a finite structure, one has to require the system to have the width of at least ten lattice periods or more. Hence, the desirable OL should be created by the beam with the highest possible frequency. In our case, there are only two electromagnetic waves in the system, which provide the transitions  $1 \leftrightarrow 2$  and  $3 \leftrightarrow 2$ , respectively. Thus we are interested in the geometry where the strong control field connects the ground  $|1\rangle$  and the excited  $|2\rangle$  states, while the probe weak wave links the states  $|1\rangle$  and  $|3\rangle$ . In the case of the strontium atoms [22] the wavelength of the probe laser beam is  $\lambda_p = 52 \mu\text{m}$  while the length of the coupling field is  $\lambda_c = 689 \text{ nm}$ . Requiring the modulation of the nonlinear polarization to have at least 20 lattice periods, we conclude that the width of the waveguide should be of order of  $14 \mu\text{m}$ .

### B. The geometry of the system

Now we can describe the geometry of the system at hand as shown in Fig. 1. The waveguide created by two parallel Bragg mirrors is placed in the  $(x, z)$ -plane. A strong control field consisting of a superposition of counter-propagating waves with the frequency  $\omega_c$  and the wavevectors  $\mathbf{k}_c \pm \mathbf{k} = (0, 0, k_c) \pm (k, 0, 0)$  ( $k \ll k_c$ ), couples the excited state  $|2\rangle$  and the ground state  $|1\rangle$ . The excited state  $|2\rangle$  is also coupled to the low energy state  $|3\rangle$  by a weak probe field of the frequency  $\omega_p$  and the wavevector  $\mathbf{k}_p = (0, 0, k_p)$  (i. e. it propagates along  $z$ -axis). We consider a planar waveguide with the transverse (i.e. along  $y$ -axis) width small enough so that only one transverse mode of the probe beam needs to be considered (see Appendix A). We concentrate on the 0-th mode designated as  $s_0(y)$ . Therefore the probe field can be presented in the form

$$\mathbf{E}_p(\mathbf{r}, t) = \mathbf{e}_p \mathcal{E}_p(x, z) s_0(y) e^{i(k_p z - \omega_p t)} + \text{c.c.} \quad (1)$$

where,  $\mathbf{e}_p$  is the polarization vector and  $\mathcal{E}_p(x, z)$  is the slowly varying envelope of the probe field.

The frequency (amplitude) of the control field  $\omega_c$  ( $E_c(\mathbf{r}, t)$ ) is much higher than that of the guided probe beam  $\omega_p$  ( $E_p(\mathbf{r}, t)$ ). This leads to a the effective refractive index of the Bragg mirrors for the control field in the claddings to be of order one (see Appendix A), allowing us neglecting its transverse distribution (we however emphasize that this design is introduced only for the sake of simplicity). The control field can be presented in the form

$$\mathbf{E}_c(\mathbf{r}, t) = 2\mathbf{e}_c \mathcal{E}_c(x, z) f(x) \cos(kx) e^{i(k_c z - \omega_c t)} + \text{c.c.} \quad (2)$$

Here,  $\mathbf{e}_c$  stands for the polarization vector, the function  $f(x)$  describes the slowly varying distribution of the control field in the  $x$  direction, and  $\mathcal{E}_c(x, z)$  is the complex amplitude of the control field. In experiments, the desired space dependence of  $f(x)$  can be achieved with the help of beam masks.

The total electric-field can be written down as  $\mathbf{E}(\mathbf{r}, t) = \mathbf{E}_p(\mathbf{r}, t) + \mathbf{E}_c(\mathbf{r}, t)$  and considered classically. Large difference between the frequencies of the probe and control fields ( $\omega_c \gg \omega_p$ ) allows us to split the equations for  $\mathbf{E}_p$  and  $\mathbf{E}_c$ , while large difference in the field amplitudes ( $E_c \gg E_p$ ) allows us to consider  $\mathbf{E}_c$  to be constant in the equation for the probe beam [8]. Now the equation governing  $\mathbf{E}_p$  can be written down as follows:

$$\left( \nabla^2 - \frac{1}{c^2} \frac{\partial^2}{\partial t^2} \right) E_p = \frac{1}{\epsilon_0 c^2} \frac{\partial^2}{\partial t^2} P. \quad (3)$$

Here  $P$  is the probe beam polarization defined by the properties of the atomic gas in the waveguide core and by the properties of the Bragg mirrors in the waveguide claddings, i.e.

$$P = \begin{cases} P_{\text{clad}}, & (y < -b, y > b) \\ P_{\text{core}}, & (-b < y < b) \end{cases} \quad (4)$$

Following the standard procedure [23]  $P_{\text{clad}}$  can be determined by calculating the effective refractive index of the Bragg mirrors  $n$  from Eq. (A3):  $P_{\text{clad}} = \epsilon_0(n^2 - 1)E_p$ .

### C. Nonlinear Polarization

In order to compute  $P_{\text{core}}$  one introduces the bosonic field operators  $\hat{\psi}_j, \hat{\psi}_j^\dagger$  of the states  $|j\rangle$  ( $j = 1, 2, 3$ ), as well as the electric dipole matrix elements  $p_{ij}$  associated with the transitions between the states  $|i\rangle$  and  $|j\rangle$ . Then the polarization can be obtained as

$$P_{\text{core}} = p_{32} \langle \hat{\psi}_3^\dagger \hat{\psi}_2 \rangle e^{i(k_p x - \omega_p t)} + \text{c.c.} \quad (5)$$

The steering of the light we are interested in is performed through the proper spatial and/or temporal modulations of  $P_{\text{core}}$ . In order to link it directly to the probe field  $E_p$  we have to address the Heisenberg equations for the operators  $\hat{\psi}_j$  describing the atomic medium. This can be done neglecting the atomic kinetic energy, what leads to the system as follows (its derivation repeats the steps outlined say in [17])

$$i \frac{\partial}{\partial t} \hat{\psi}_1 = -\Delta_1 \hat{\psi}_1 - 2\Omega_c^* f(x) \cos(kx) \hat{\psi}_2, \quad (6a)$$

$$i \frac{\partial}{\partial t} \hat{\psi}_2 = (\Delta_2 - i\gamma_2) \hat{\psi}_2 - 2\Omega_c f(x) \cos(kx) \hat{\psi}_1 - \Omega_p \hat{\psi}_3, \quad (6b)$$

$$i \frac{\partial}{\partial t} \hat{\psi}_3 = -\Omega_p^* \hat{\psi}_2. \quad (6c)$$

Here  $\Omega_p = p_{23} \mathcal{E}_p / \hbar$  and  $\Omega_c = p_{21} \mathcal{E}_c / \hbar$ , are the Rabi frequencies of the respective fields  $\Delta_2 = (\omega_2 - \omega_3) - \omega_p$ , and  $\Delta_1 = (\omega_3 - \omega_1) - (\omega_c - \omega_p)$  present one- and two-photon detunings, respectively (see Fig. 1). In Eqs. (6), we keep only the dissipation of the state  $|2\rangle$  due to spontaneous emission, by adding the decay rate  $\gamma_2$ , phenomenologically. Usually, the decay rates of the lower states  $|1\rangle$  and  $|3\rangle$  are much smaller than that of the excited state and can be safely neglected. For a particular choice of the atomic gas and assuming that the decay rate of the excited state is much less than the two-photon detuning ( $\gamma_2 \ll \Delta_1$ ), one may consider the loss of the atoms from the system as a small perturbation (see also the discussion in [17]).

Since the two-photon detuning is nonzero (i.e.  $\Delta_1 \neq 0$ ), the pure dark state (corresponding to  $\hat{\psi}_2 \equiv 0$ ) can not exist. However, we explore the situation where the atomic system is close enough to the dark state. To this end we look for a solution of Eqs. (6) in the form  $\hat{\psi}_j(\mathbf{r}, t) = e^{i\lambda t} \hat{\phi}_j(\mathbf{r})$ , where the exponent  $\lambda$  is slowly varying in space and can be obtained as a root of the respective characteristic equation. We are interested in a root having the smallest imaginary part [24], i.e.

$$\lambda = \lambda_r + i\lambda_i, \quad (7)$$

( $|\lambda_i| \ll |\lambda_r|$ ) with

$$\lambda_r = \frac{\Delta_1 |\Omega_p|^2}{\Delta_1 \Delta_2 + 4|\Omega_c|^2 f^2(x) \cos^2(kx) + |\Omega_p|^2},$$

$$\lambda_i = \frac{\gamma_2}{|\Omega_p|^2} \lambda_r^2.$$

Then the expectation value  $\langle \hat{\psi}_3^\dagger \hat{\psi}_2 \rangle$  can be readily computed from (6) and (7):

$$\langle \hat{\psi}_3^\dagger \hat{\psi}_2 \rangle = \frac{\Lambda |\delta_1 - \Lambda|^2 \Omega}{(|\Lambda|^2 + |\Omega|^2) |\delta_1 - \Lambda|^2 + 4|\Lambda|^2 f^2(x) \cos^2(kx)}. \quad (8)$$

Here we introduced the dimensionless functions  $\Omega = \Omega_p / \Omega_c$  and

$$\Lambda = \frac{\lambda}{|\Omega_c|} = \Lambda_r + i\Lambda_i, \quad (9)$$

where

$$\Lambda_r = \frac{\delta_1 |\Omega|^2}{\delta_1 \delta_2 + 4f^2(x) \cos^2(kx) + |\Omega|^2},$$

$$\Lambda_i = \frac{\tilde{\gamma}_2}{|\Omega|^2} \Lambda_r^2,$$

as well as the parameters  $\delta_j = \Delta_j / |\Omega_c|$  ( $j = 1, 2$ ) and  $\tilde{\gamma}_2 = \gamma_2 / |\Omega_c|$ . Since the probe field (decay rate of the excited state) is assumed to be weak in comparison with the control field, we have that  $|\Omega| \ll 1$  ( $\tilde{\gamma}_2 \lesssim |\Omega|^2 \ll 1$ , see Eq. (11) and the related discussions).

An important conclusion follows from Eq. (6c), the quasi-dark state, characterized by the small population

of the excited state  $|2\rangle$ , requires  $|\lambda| \ll |\Omega_p|$  and hence  $|\Lambda| \ll 1$ .

In what follows we will be interested in a particular choice  $f(x) = 1 - ax$  where  $a$  is the mask parameter considered to be small. More specifically, we will consider the beam propagation (i.e. distributions of  $\Omega$  in space) characterized by finite deviations from the axis  $x$ . As we have already announced in the Introduction, the mentioned deviation will occur due to BOs of the beam. Thus if we assume that the amplitude of BOs measured in units  $k^{-1}$  [see Eq. (13) below] is  $X$ , the smallness of  $a$  is determined by the requirement that  $aX/k \sim \Omega^2 \ll 1$ . This allows us to achieve further simplification for the polarization by defining

$$v(kx) \equiv \delta_1 \delta_2 + 4 \cos^2(kx). \quad (10)$$

Performing the expansion of the right hand side of Eq. (8) in the Taylor series with respect to  $\Omega$  we get:

$$\begin{aligned} \langle \hat{\psi}_3^\dagger \hat{\psi}_2 \rangle \simeq & \frac{\delta_1 \Omega}{v(kx)} \left[ 1 + \frac{8ax \cos^2(kx)}{v(kx)} \right. \\ & \left. - \frac{\delta_1^2 - \delta_1 \delta_2 + 2v(kx)}{v(kx)^2} |\Omega|^2 \right] + i \frac{\delta_1^2 \tilde{\gamma}_2}{v(kx)^2} \Omega. \end{aligned} \quad (11)$$

Here we have neglected the  $\Omega^5$ -order terms and assumed that in the domain of BOs the condition  $|\Omega|^2 \ll v(x)$  is satisfied. Notice that the requirement  $v(x) \neq 0$  holds for in the whole space provided

$$\delta_1 \delta_2 > 0 \quad \text{or} \quad \delta_1 \delta_2 < -4. \quad (12)$$

This condition will be imposed in what follows.

#### D. The equation for the beam envelope

We are particularly interested in the beam dynamics resulting from the interplay of diffraction and nonlinearity when the probe field passes through the atomic cloud. Therefore, we concentrate on stationary solutions, requiring  $\Omega$  to be independent on time. Substituting Eqs. (1) and (11) into Eq. (3), taking into account (A1), and leaving only the leading order terms, we arrive at the dimensionless equation for the slowly varying function  $\Omega$ :

$$\begin{aligned} i \frac{\partial \Omega}{\partial \zeta} + \frac{\partial^2 \Omega}{\partial \xi^2} + U(\xi) \Omega + \xi F(\xi) \Omega - G(\xi) |\Omega|^2 \Omega \\ + i \Gamma(\xi) \Omega = 0. \end{aligned} \quad (13)$$

Here  $\xi = kx$  and  $\zeta = (k^2/2k_p)z$  are the dimensionless independent variables,  $v(\xi) = v(kx)$  is given by (10), and we defined

$$\begin{aligned} U(\xi) &= \frac{U_0}{v(\xi)}, \quad F(\xi) = \frac{8a'U_0 \cos^2(\xi)}{v^2(\xi)}, \\ G(\xi) &= \frac{C_0 U_0 [\delta_1^2 - \delta_1 \delta_2 + 2v(\xi)]}{v^3(\xi)}, \quad \Gamma(\xi) = \frac{\delta_1 \tilde{\gamma}_2 U_0}{v(\xi)^2}, \end{aligned}$$

with

$$U_0 = \frac{\mathcal{N} |\mathbf{p}_{32}|^2 k_p^2}{\hbar \epsilon_0 k^2 \Omega_c} \delta_1,$$

and  $a' = a/k$ . The constant  $C_0$  depending on the particular choice of the Bragg mirrors is computed in the Appendix A.

The obtained dimensionless Eq. (13) implies that all the terms are of the order one or less. More specifically, it is necessary to require that  $U_0 \sim 1$ . This last constrain can be satisfied by different means. Notice that the parameter  $k_p/k$  can be experimentally controlled by the geometry of the laser beams (see Fig. 1), we thus fix  $k_p/k = 0.2$  and adjust other parameters (in particular  $\delta_1$  and  $\Omega_c$ ) to satisfy the constrain. For a typical set of data explored below, i.e. the atomic concentration  $\mathcal{N} \approx 10^{14} \text{ cm}^{-3}$  and  $\Delta_1 = \Omega_c = 1.0 \times 10^7 \text{ s}^{-1}$  ( $\delta_1 = 1$ ), we obtain  $U_0 = 4.7$  satisfying the desired order of magnitude. Meanwhile, the dissipation is very small ( $\Gamma(\xi) \ll 1$ ) in the considered system since  $\tilde{\gamma}_2 = 4.7 \cdot 10^{-3} \ll 1$ .

### III. SPATIAL GAP SOLITONS AND ALL-OPTICAL STEERING

#### A. Spatial gap solitons

We study the situation when the effects of the linear force, nonlinearity, and dissipation are small enough. Therefore we first notice that for  $F \equiv 0$ ,  $G \equiv 0$ , and  $\Gamma \equiv 0$  one arrives at the familiar framework of the band theory, where by means of substitution  $\Omega \propto e^{-iK_\alpha \zeta}$  Eq. (13) is reduced to the eigenvalue problem

$$\hat{\mathcal{L}} u_{\alpha,q}(\xi) + K_\alpha(q) u_{\alpha,q}(\xi) = 0. \quad (14)$$

Here  $\hat{\mathcal{L}} = -\partial^2/\partial \xi^2 - U(\xi)$  and  $u_{\alpha,q}(\xi)$  is a Bloch function with indexes  $\alpha$  and  $q$  standing respectively for the band index and for the wave vector in the first Brillouin zone (BZ), i.e. for  $q \in [-1, 1]$  in the case at hand. The physical meaning of the eigenvalue  $K_\alpha(q)$  is the propagation constant. In what follows we concentrate on the lowest energy band ( $\alpha = 0$ ) and therefore, for the sake of brevity, omit the band index.

The effect of the periodic linear force originated by the control beam can be described by the equations

$$\frac{d\Xi}{d\zeta} = \tan \theta = \frac{dK_\alpha(Q)}{dQ}, \quad \frac{dQ}{d\zeta} = -F(\Xi), \quad (15)$$

where  $\Xi$  and  $Q$  denote the coordinates of the center of the Bloch wave packet in the real and reciprocal spaces, respectively.  $\theta$  is the refraction angle with  $\tan \theta = 2(k_p/k) \tan \theta_p$  (see Figs. 1 (a) and 3 (a)). A peculiarity of our case is that  $F(\xi)$  is an oscillating function, which has a nonzero mean value

$$\langle F \rangle = \frac{1}{\pi} \int_0^\pi F(\xi) d\xi = \frac{4a'U_0}{|\delta_1 \delta_2 + 4| \sqrt{(\delta_1 \delta_2 + 4) \delta_1 \delta_2}},$$

and hence results in the oscillation behavior of the Bloch wave packet in the real and reciprocal spaces (i.e. in BOs). The dimensionless amplitude (along the  $x$  axis) and period (along the  $z$  axis) of such oscillations can be calculated as  $X = \Delta K/2\langle F \rangle$ , with  $\Delta K$  denoting the width of the lowest allowed band of the periodic potential  $U(\xi)$ , and  $Z = 2/|\langle F \rangle|$ , respectively.

In order to describe the effect of the nonlinearity we employ the standard multiple-scale expansion assuming smallness of the averaged force, i.e.  $\langle F \rangle \ll 1$ . This last requirement is equivalent to the condition  $a \ll k$ , which is consistent with the constrains on the BOs amplitude discussed in Sec. II C provided  $X \lesssim 1$ .

Next we introduce the scaled variables  $(\xi_j, \zeta_j) \equiv \mu^{j/2}(\xi, \zeta)$  ( $j = 1, 2, \dots$ ), where  $\mu$  is a small parameter estimated by  $\mu \sim \langle F \rangle \ll 1$ . The probe field can be written in the form of the expansion  $\Omega = \sum_{j=1}^{\infty} \mu^{j/2} \Omega^{(j)}(\xi_0, \zeta_1)$ , where in the arguments of the functions  $\Omega^{(j)}$  we have indicated only the most rapid variables.  $\Gamma(\xi) = \mu^2 \mathcal{R}(\xi_0)$ . Substituting this ansatz into Eq. (13) and collecting the terms at each order of  $\mu^{1/2}$ , we obtain a set of equations which can be solved order by order (see e.g. [25]). Omitting the details we turn directly to the equation for the slowly varying amplitude  $A(\chi, \zeta_2)$ , which is defined through the relation  $\Omega^{(1)} = A(\chi, \zeta_2) e^{iK(Q)\zeta_0} u_Q(\xi_0)$ , where  $\chi = \xi_1 - \tan[\theta(\zeta_2)] \zeta_1$  and the dependence  $Q = Q(\zeta_2)$  and  $\theta(\zeta_2)$  are obtained from Eqs. (15). In the third order of the asymptotic expansion,  $\mathcal{O}(\mu^{3/2})$ , we obtain

$$i \frac{\partial A}{\partial \zeta_2} + \mathcal{D}(Q) \frac{\partial^2 A}{\partial \chi^2} - \mathcal{G}(Q) |A|^2 A + i \mathcal{R}(Q) A = 0, \quad (16)$$

where the coefficients of the diffraction  $\mathcal{D}$  and the effective nonlinearity  $\mathcal{G}$  are given respectively by

$$\mathcal{D}(Q) = \frac{1}{2} \frac{d^2 K(Q)}{dQ^2}, \quad \mathcal{G}(Q) = \int_0^\pi G(\xi) |u_Q(\xi)|^4 d\xi,$$

$$\mathcal{R}(Q) = \int_0^\pi \mathcal{R}(\xi) |u_Q(\xi)|^2 d\xi.$$

We notice that both  $\mathcal{D}$  and  $\mathcal{G}$  can be either positive or negative depending on the signs of detunings and on the position of the center of the wave packet (i.e. on  $\zeta_2$ ). Therefore, in a general case BOs oscillations will be accompanied by significant change of the width of the beam, due to the diffraction. This undesired effect, however can be dramatically reduced, if the conditions for self-focusing of the beam will be satisfied (and hence will compensate the diffraction) at any coordinate  $\zeta_2$ . These requirements (which are also referred to as conditions for the gap soliton existence or, alternatively, as conditions of the modulational instability of the Bloch waves), are well known and read [25, 26]

$$\mathcal{D}(Q)\mathcal{G}(Q) < 0. \quad (17)$$

If condition (17) is satisfied for all (or almost all) wavevectors  $Q$ , the self-focusing of the beam will occur along the whole (or almost whole) trajectory of the beam.

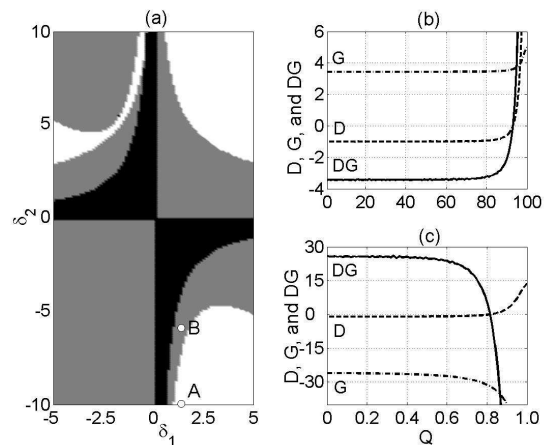


FIG. 2: (a) The white domains correspond to the choice of the detuning, such that (17) is valid for 90% of wavevectors in the first BZ; in the black domains the requirement (12) is not satisfied and thus the approximation Eq. (13) fails; the gray domains show the parameter region where our approximation is valid, but the conditions (17) are not satisfied for more than 10% of the wavevectors in the BZ. The system parameters are given in Sec. II A. (b) The coefficients  $\mathcal{D}(Q)$  (dashed line),  $\mathcal{G}(Q)$  (dash-dotted line), and  $\mathcal{D}(Q)\mathcal{G}(Q)$  (solid line) vs  $Q$  with the parameters  $U_0 = 4.7$ ,  $\Delta_1 = \Omega_c = 1.0 \times 10^7 \text{ s}^{-1}$ , and  $\Delta_2 = -1.0 \times 10^8 \text{ s}^{-1}$  [the point A in panel (a)]. (c) The same as in panel (b) but with  $\Delta_2 = -0.6 \times 10^8 \text{ s}^{-1}$  [the point B in panel (a)]. The dynamics of the Bloch wave packets for the points A and B is shown below in the panels (a) and (b) of Fig. 3.

Thus, as the third step, for achieving the best performance of the device one has to design the system (geometry of the beams or photon detunings) in a way to ensure the condition (17) for all  $Q$ . The procedure of performing this task was described in the previous works [18, 26] and here we report only the final result. More specifically, in Fig. 2 (a), we show the domains on the plain  $(\delta_1, \delta_2)$  where the optimal conditions are satisfied (empty regions), not satisfied (gray regions), and the parameter requirement (12) is violated (black regions). In Fig. 2 (b) and (c), we plot the curves  $\mathcal{D}(Q)$ ,  $\mathcal{G}(Q)$ , and  $\mathcal{D}(Q)\mathcal{G}(Q)$  versus  $Q$  with the almost optimal design [point A in panel (a)] and non optimal design [point B in panel (a)] of the OLs. We mention that always there exists a small range of the wavevectors where spatial gap solitons do not exist (i.e. where  $\mathcal{D}(Q)\mathcal{G}(Q) > 0$ ). This range, however, can be made enough small [less than 10% of the whole BZ, like this happens in the point A, see Fig. 2 (b)], and therefore has no appreciable destructive effect on the beam dynamics [see Fig. 3 (a)]. On the contrary, the point B in panel (a) corresponds to the case in which the BOs of the beam are rapidly destroyed leading to strong defocussing of the outcome beam [see Fig. 3 (b)].

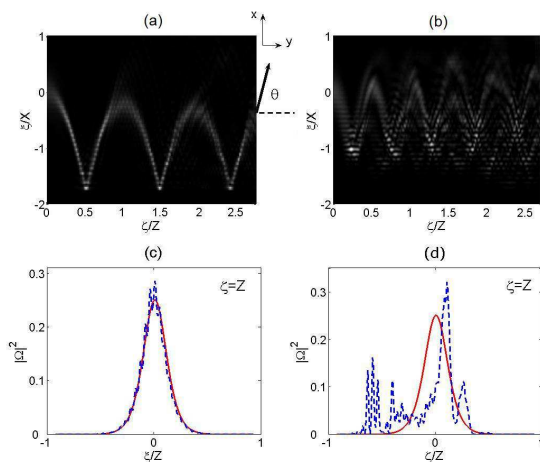


FIG. 3: (color on line) (a) The long-living BOs of the beam in the almost optimally designed OLs [point *A* in Fig. 2 (a)] obtained by direct numerical integration of Eq. (13). The amplitude and the period of the BOs are  $X = 14.47$  ( $= 49 \mu\text{m}$ ) and  $Z = 578.98$  ( $= 787 \mu\text{m}$ ). (b) BOs of the wave packet in the non optimally designed OLs [point *B* in Fig. 2 (a)]. In the both cases the initial condition is a stationary gap soliton located at  $\xi/X = 0$ . The intensity profiles of the output beam (blue, dashed line) vs the input beam (red, solid line) corresponding to the cases (a) and (b) are respectively shown in the panels (c) and (d) obtained at  $\zeta = Z$ .

### B. Long-living BOs and all-optical steering

Now we turn to the final step of numerical descriptions of the BOs of a spatial soliton and of the light steering. In Fig. 3 (a), we show the dynamics of the Bloch wave packet launched normally in the atomic media with the almost optimal design of the OLs [point *A* in Fig. 2 (a)]. The result was obtained by employing numerical integration of Eq. (13). The existence of the long-living BOs of the gap soliton, with the amplitude and period well matching the theoretical estimates, can be observed. Due to the very small dissipation, there is only a tiny decrease of the soliton intensity due to the absorption of the medium. More specifically, one can see the highly concentrated beam in the output with the direction of propagation determined by the nonzero angle  $\theta$ . For the sake of comparison, in Fig. 3 (b), we show the dynamics of the same Bloch wave packet in the non optimally designed OL [The parameters used in this panel are the same with those used in Fig. 2 (c)]. In this case, the beam undergoes strong spreading out due to the alternating diffractive and self-defocussing regeems. The intensity profiles of the output beam vs the input beam are shown in the panels (c) and (d). One observes that there is no apparent deformation between the output beam and input beam in panel (c) while an obvious destruction appears in panel (d).

The maximum input intensity of the probe beam in Fig. 3 (a) can be estimated by the formula  $I_{\text{max}} =$

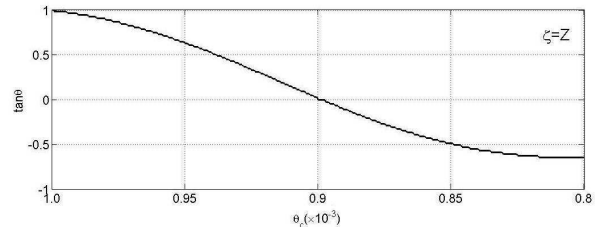


FIG. 4:  $\tan \theta$  vs  $\theta_c$  at  $\zeta = Z$  for the almost optimally designed OLs [corresponding to point *A* in Fig. 2 (a) and panel (a) of Fig. 3].

$(c/2)\epsilon_0|\mathbf{E}_{p \text{ max}}|^2$ . Using the parameters given in Fig. 2 (b), we obtain  $I_{\text{max}} \approx 4.5 \mu\text{W cm}^{-2}$ . Thus, the generation of the spatial gap soliton in the system at hand requires only very low input light intensity. We remark that the intensity of a single 500-nm photon per nanosecond on an area of  $1 \mu\text{m}^2$  is  $I_{ph} = 0.04 \text{ W cm}^{-2}$ . This estimation shows that our system makes it possible to manage the weak beams characterized by single-photon wavepackets. This is drastically different from the spatial optical soliton generation in a conventional waveguide where an input laser pulse with very high peak power  $\sim 10^2 \text{ kW}$  is needed in order to bring out a sufficient nonlinear effect [27].

The existence of long-living BOs of spatial optical gap solitons can be used to implement efficient all-optical steering of probe beams. Different from all linear systems where the spread and attenuation of the probe pulse are unavoidable because the refractive index gradient depends on both light frequency and spatial coordinates, the scheme proposed here can greatly improve the device performance due to the self-focusing of the beam. In experiments, the optical masks and atomic cells are usually chosen in advance. However, one can exploit the possibility of changing the geometry or parameters of the control field to steer the output probe beam. As an example, by changing the angle between the input control fields  $\theta_c = \arctan(k/k_c)$  (see Fig. 1), one can efficiently control the refraction angle of the output probe beam. In Fig. 4, we show the tangent of the refraction angle  $\tan \theta$  versus  $\theta_c$  with a particular length of atomic cells (i.e.  $\zeta = Z$ ). A wide range of angle,  $\theta_p \in [-0.98, 1.19]$ , can be achieved with the given parameters.

## IV. CONCLUSION

In conclusion, we studied (both analytically and numerically) the dynamics of weak probe optical beams in a gas of three-level  $\Lambda$ -atoms subjected to a control laser beam. The standing wave originates periodic modulations of the linear and nonlinear parts of the dielectric permittivity of the medium, which is “seen” by the probe

beam. If the amplitude of the control field is smoothly modulated, the probe beam undergoes the Bloch oscillations. These oscillations correspond to periodic change of the direction of the propagation of the beam. We have shown that it is possible to choose the parameters of the atomic system, say Rabi frequency of the control field and photon detunings, to reduce the diffraction of the probe beam, and thus the output beam is approximately the same with the input one. In this case, the probe field distributions is nothing but a spatial gap soliton undergoing long-living Bloch oscillations. Due to the significant enhancement of nonlinearity, such solitons can be formed with extremely weak light intensity, below single-photon wavepacket level. Thus, through changing the geometry or parameters of the system one can control the direction of the output beam to carry out an efficient all-optical steering of light.

### Acknowledgments

The work of C.H. was supported by the Fundação para a Ciência e a Tecnologia (FCT) under Grant No. SFRH/BPD/36385/2007 and Estímulo à Investigação 2009 de Fundação Calouste Gulbenkian. The research of VVK was partially supported by the grant PIIF-GA-2009-236099 (NOMATOS).

### Appendix A: The transverse profiles of the probe field

The transverse profiles of the probe field can be determined from the eigenvalue problem [23]

$$\left(\frac{\partial^2}{\partial y^2} + \frac{\omega^2}{c^2} - k_l^2\right) s_l(y) = 0, (|y| < b) \quad (\text{A1a})$$

$$\left(\frac{\partial^2}{\partial y^2} + \frac{n^2\omega^2}{c^2} - k_l^2\right) s_l(y) = 0, (|y| > b) \quad (\text{A1b})$$

where  $\omega$  stands for either  $\omega_p$  or  $\omega_c$ ,  $l$  stands for the mode index ( $l = 0, 1, \dots$ ),  $s_l(y)$  is a normalized, i.e.

$\int_{-\infty}^{\infty} dy |s_l(y)|^2 = 1$ , profile of the respective mode, and  $2b$  is the width of the waveguide core.

The eigenvalue  $k_l$  and effective refractive index of the Bragg mirrors  $n$  can be obtained from the dispersion relations of the planar waveguide

$$\tan^2 \left[ b \sqrt{\frac{\omega^2}{c^2} - k_l^2} - \frac{(l+1)\pi}{2} \right] = \frac{k_l^2 c^2 - \omega^2}{n^2 \omega^2 - k_l^2 c^2}, \quad (\text{A2})$$

and the expression valid the finite photonic structures [28]

$$n(\omega) = \frac{c}{\omega h} \left( \phi_t - \frac{i}{2} \ln T(\omega) \right), \quad (\text{A3})$$

where  $\phi_t(\omega)$  and  $T(\omega)$  are the total phase and the transmittance of the complex transmission coefficient for the structure  $t(\omega) = x(\omega) + iy(\omega) = \sqrt{T} e^{i\phi_t}$  with  $\phi_t = \arctan(y/x) \pm m\pi$  (the integer  $m$  is uniquely defined assuming  $\phi_t$  is a monotonically increasing function) and  $T(\omega) = x^2 + y^2$ .  $h$  is the total thickness of the  $N$ -period crystal  $h = N(h_a + h_b)$  with  $h_a$  and  $h_b$  being the thicknesses of two different materials [see Fig. 1 (b)].

As an example we consider the probe field constrained of quarter-wave Bragg mirrors,  $n_a h_a = n_b h_b = \lambda_p/4$  with  $n_a = 1.0$  and  $n_b = 1.4$  being the refractive indexes of the two different materials, for claddings,  $N = 2$ , and  $2b = 0.1$  mm, we obtain that  $k_0 = 1081 \text{ cm}^{-1}$  and  $n \approx 0.87$ . At the same time, for the control field we have  $k_0 \approx 91144 \text{ cm}^{-1}$  and the effective refractive index of the cladding is  $n \approx 1.0$ .

The assumption that only  $s_0$  takes into account requires that the energy for exciting  $s_1$  [corresponding to the eigenvalue of Eq. (A1a)] is higher than that of the self-action (nonlinearity) in Eq. (13). With the parameters given in Fig. 2, we obtain  $G(\xi)|\Omega|^2\Omega < (\omega_p^2/c^2 - k_1^2)/k^2$  ( $k_1 = 873 \text{ cm}^{-1}$  for the probe field), hence we can safely neglect the higher transverse modes (i.e.  $s_l$  for  $l > 0$ ). Here, the integral  $C_0 = \int_{-\infty}^{\infty} |s_0|^4 d\eta = 73.9$ . However, the much higher frequency of the control field allows us to neglect the difference among transverse profiles of the control field in the waveguide core.

- 
- [1] V. J. Fowler and J. Schlafer, Proc. IEEE **54**, 1437 (1966); M. Gottlieb, C. L. M. Ireland, and J. M. Ley, *Electro-Optic and Acousto-Optic Scanning and Deflection* (Dekker, New York, 1983).
- [2] I. Cindrich, Appl. Opt. **6**, 1531 (1967); D. H. McMahon, A. R. Franklin, and J. B. Thaxter, Appl. Opt. **8**, 399 (1969).
- [3] W. B. Jackson, N. M. Amer, A. C. Boccara, and D. Fournier, Appl. Opt. **20**, 1333 (1981).
- [4] R. W. Dixon, J. Appl. Phys. **38**, 5149 (1967); D. A. Pinnow, IEEE J. Quantum Electron. **6**, 223 (1970).
- [5] E. G. Spencer, P. V. Lenzo, and A. A. Ballman, Proc. IEEE **55**, 2074 (1967); T. C. Lee and J. D. Zook, IEEE J. Quantum Electron. **4**, 442 (1968); J. F. Lotspeich, IEEE Spectrum **5**, 45 (1968); J. D. Zook, Appl. Opt. **13**, 875 (1974); D. Scrymgeour, N. Malkova, S. Kim, and V. Gopalan, App. Phys. Lett., **82**, 3176 (2003).
- [6] H. Kosaka, T. Kawashima, A. Tomita, M. Notomi, T. Tamamura, T. Sato, and S. Kawakami, Phys. Rev. B **58**, 10096 (1998); T. Baba and M. Nakamura, IEEE J. Quantum Electron. **38**, 909 (2002).
- [7] F. Vasey, F. K. Reinhart, R. Houdre, and J. M. Stauffer, Appl. Opt. **32**, 3220 (1993); M. W. Farn, Appl. Opt. **33**, 5151 (1994).
- [8] S. E. Harris, Phys. Today **50**, 36 (1997); M. Fleischhauer, A. Imamoglu, and J. P. Marangos, Rev. Mod. Phys. **77**,

- 633 (2005).
- [9] S. E. Harris, J. E. Field, and A. Imamoglu, Phys. Rev. Lett. **64**, 1107 (1990); M. O. Scully and S. Y. Zhu, Opt. Commun. **87**, 134 (1992); M. Xiao, Y. Q. Li, S. Z. Jin, and J. Gea-Banacloche, Phys. Rev. Lett. **74**, 666 (1995).
- [10] G. T. Purves, G. Jundt, C. S. Adams, and I. G. Hughes, Eur. Phys. J. D **29**, 433 (2004).
- [11] R. Holzner, P. Eschle, S. Dangel, R. Richard, H. Schmid, U. Rusch, B. Röhrich, R. J. Ballagh, A. W. McCord, and W. J. Sandle, Phys. Rev. Lett. **78**, 3451 (1997); D. L. Zhou, L. Zhou, R. Q. Wang, S. Yi, and C. P. Sun, Phys. Rev. A **76**, 055801 (2007).
- [12] Q. Sun, Y. V. Rostovtsev, and M. S. Zubairy, Phys. Rev. A **74**, 033819 (2006).
- [13] R. R. Moseley, S. Shepherd, D. J. Fulton, B. D. Sinclair, and M. H. Dunn, Phys. Rev. Lett. **74**, 670 (1995); A. G. Truscott, M. E. J. Friese, N. R. Heckenberg, and H. Rubinsztein-Dunlop, Phys. Rev. Lett. **82**, 1438 (1999); R. Kapoor and G. S. Agarwal, Phys. Rev. A **61**, 053818 (2000); J. A. Andersen, M. E. J. Friese, A. G. Truscott, Z. Ficek, P. D. Drummond, N. R. Heckenberg, and H. Rubinsztein-Dunlop, Phys. Rev. A **63**, 023820 (2001).
- [14] H. Schmidt and A. Imamoglu, Opt. Lett. **21**, 1936 (1996); D. Petrosyan and G. Kurizki, Phys. Rev. **65**, 033833 (2002).
- [15] Y. Wu and L. Deng, Phys. Rev. Lett. **93**, 143904 (2004); G. Huang, L. Deng, and M. G. Payne, Phys. Rev. E **72**, 016617 (2005); C. Hang, G. Huang, and L. Deng, Phys. Rev. E **73**, 036607 (2006).
- [16] H. Michinel and M. J. Paz-Alonso, and V. M. Pérez-García Phys. Rev. Lett. **96**, 023903 (2006); C. Hang, G. Huang, and L. Deng, Phys. Rev. E **73**, 046601 (2006).
- [17] C. Hang, V. V. Konotop, and G. Huang, Phys. Rev. A **79**, 033826 (2009).
- [18] M. Salerno, V. V. Konotop, and Yu. V. Bludov, Phys. Rev. Lett. **101**, 030405 (2008).
- [19] S. Ghosh, A. R. Bhagwat, C. K. Renshaw, S. Goh, A. L. Gaeta, and B. J. Kirby, Phys. Rev. Lett. **97**, 023603 (2006); P. S. Light, F. Benabid, F. Couny, M. Maric, and A. N. Luiten, Opt. Lett. **32**, 1323 (2007); T. Takekoshi and R. J. Knize, Phys. Rev. Lett. **98**, 210404 (2007); C. A. Christensen, S. Will, M. Saba, G. Jo, Y. Shin, W. Ketterle, and D. Pritchard, Phys. Rev. A **78**, 033429 (2008).
- [20] S. Ghosh, J. E. Sharping, D. G. Ouzounov, and A. L. Gaeta, Phys. Rev. Lett. **94**, 093902 (2005).
- [21] M. Bajcsy, S. Hofferberth, V. Balic, T. Peyronel, M. Hafezi, A. S. Zibrov, V. Vuletic, and M. D. Lukin, Phys. Rev. Lett. **102**, 203902 (2009).
- [22] A. Traverso, R. Chakraborty, Y. N. Martinez de Escobar, P. G. Mickelson, S. B. Nagel, M. Yan, and T. C. Killian, Phys. Rev. A **79**, 060702 (2009).
- [23] J. Heebner, R. Grover, and T. Ibrahim, *Optical Microresonators* (Springer Series in Optical Sciences, Vol. 138, 2008).
- [24] The two other roots describe fast decay of the respective expectation values and therefore not considered here.
- [25] V. V. Konotop and M. Salerno, Phys. Rev. A **65**, 021602(R) (2002).
- [26] Yu. V. Bludov and V. V. Konotop Phys. Rev. A **74**, 043616 (2006); Yu. V. Bludov, V. A. Brazhnyi, and V. V. Konotop, Phys. Rev. A **76**, 023603 (2007)
- [27] J. S. Aitchison, A. M. Weiner, and Y. Silberberg, Opt. Lett. **15**, 471 (1990).
- [28] M. Centini, C. Sabilia, M. Scalora, G. D'Aguanno, M. Bertolotti, M. J. Bloemer, C. M. Bowden, I. Nefedov, Phys. Rev. E **60**, 4891 (1999).